

LETTER

Making tissintite: Mimicking meteorites in the multi-anvil

MELINDA J. RUCKS^{1,*}, MATTHEW L. WHITAKER^{1,2}, TIMOTHY D. GLOTCH¹, JOHN B. PARISE^{1,2},
STEVEN J. JARET¹, TRISTAN CATALANO¹, AND M. DARBY DYAR³

¹Department of Geosciences, Stony Brook University, Stony Brook, New York 11794-2100, U.S.A.

²Mineral Physics Institute, Stony Brook University, Stony Brook, New York 11794-2100, U.S.A.

³Department of Astronomy, Mount Holyoke College, South Hadley, Massachusetts 01075, U.S.A.

ABSTRACT

Tissintite is a shock-induced, Ca-rich mineral, isostructural to jadeite, observed in several meteorite samples such as the martian shergottite Tissint. It may form within a “Goldilocks Zone,” indicating a potential to provide strict constraints on peak pressure and temperature conditions experienced during impact. Here we present the first laboratory synthesis of tissintite, which was synthesized using a large volume multi-anvil apparatus at conditions ranging from 6–8.5 GPa and 1000–1350 °C. For these experiments, we utilized a novel heating protocol in which we reached impact-relevant temperatures within 1 s and in doing so approximated the temperature-time conditions in a post-shock melt. We have established that heating for impact-relevant timescales is not sufficient to completely transform crystalline labradorite to tissintite at these pressures. Our findings suggest that tissintite forms from amorphous plagioclase during decompression.

Keywords: Tissintite, high-pressure, high-temperature, shock, multi-anvil

INTRODUCTION

The study of high-pressure, high-temperature phases in meteorite samples gives us insight into the impact processes that shape the evolution of planetary surfaces. High-pressure, high-temperature minerals observed within meteorites act as snapshots of the *P-T* conditions experienced by the rocks during the impact events that produced them (Chen et al. 1996; Chen and El Goresy 2000; Ohtani et al. 2004; Xie et al. 2006; Sharp and DeCarli 2006; Gillet et al. 2007; Fritz et al. 2017). However, using these phases as index minerals to determine impact conditions depends upon the availability of experimentally derived *P-T* stability field data, which do not exist for many newly discovered minerals observed in meteorites, such as tissintite.

Tissintite is reported as a non-stoichiometric clinopyroxene (Cpx), (Ca,Na,□)AlSi₂O₆, with a calcium-rich plagioclase or labradorite (~An₆₅) composition and a jadeite-type structure. It was first observed in the Martian shergottite, Tissint (Ma et al. 2014), and has since proven to be prevalent in shocked samples, including other shergottite meteorites (Herd et al. 2017), a eucrite meteorite (Pang et al. 2016), and a possible terrestrial occurrence in shock-generated melts from the Manicouagan crater (Boonsue and Spray 2017). It occurs as sub-micrometer-sized crystalline aggregates within maskelynite grains that are entrained in or adjacent to shock-generated melts with no other coexisting crystalline phases detected by Raman spectroscopy (Ma et al. 2015). Tissintite is proposed to contain approximately 25% vacancies at the M2 site, the highest concentration ever reported for either natural or synthetic Cpx; however, a refined crystal structure confirming these structural defects has not

been determined (Ma et al. 2015). Tissintite has been suggested to form within a so-called “Goldilocks Zone” where pressure, temperature, time, and composition (*P-T-t-X*) are just right to facilitate growth of the phase, thus suggesting its great potential to provide strict constraints on the *P-T* path followed during an impact event (Ma et al. 2015). Previous to this study, tissintite had never before been synthesized and little was known about the controls on its formation during an impact event.

There are several path-dependent variables that could influence the formation of tissintite during an impact event, including pressure, temperature, and time, as well as a non-path-dependent variable such as composition, and crystallinity of the precursor. Some of these have been estimated through observations of natural occurrences by Walton et al. (2014) and Ma et al. (2015). The first reported occurrence of tissintite (Ma et al. 2014) was observed within maskelynite grains of calcic-plagioclase composition while being absent in sodic-plagioclase grains. Tissintite was exclusively found in grains that abut or are entrained in >500 μm shock-generated melt veins or pockets and only within ~25 μm of the melt-grain interface. These observations indicate the following requirements for tissintite formation: (1) a calcium-rich plagioclase precursor and (2) temperatures >900 °C. Additionally, tissintite does not occur with any accompanying crystalline phases in any of the reported occurrences. This is significant because it suggests these natural occurrences of tissintite may be controlled by kinetic factors rather than pressure or temperature alone as has been suggested for other phase transformations spatially associated with shock melt such as olivine to ringwoodite (Xie et al. 2006).

Although the number of studies concerning the behavior of intermediate plagioclase compositions at elevated *P-T* is limited, we can use studies of the end-members albite and anorthite to make

* E-mail: melinda.rucks@stonybrook.edu

inferences on how these intermediate compositions may behave. At high pressure and temperature, albite and labradorite have been observed to form jadeite + stishovite at HP-HT with differing crystallization rates where jadeite crystallizes first and is subsequently followed by a crystalline silica phase after >100 s (Kubo et al. 2010). These observations, taken together with tissintite's association with melt veins and pockets (Walton et al. 2014; Ma et al. 2015), suggest that the precursor needs to be at temperature for up to ~1 s or longer (Langenhorst and Poirier 2000; Shaw and Walton 2013; Walton et al. 2014) for the plagioclase-to-tissintite transformation to occur, but not so long as to form accompanying crystalline phases. Furthermore, it is unclear from natural samples whether the precursor is crystalline plagioclase or if it is maskelynite/amorphous plagioclase. The experiments performed here were designed to approximate and test these conditions. Here we have determined an initial range of formation conditions for tissintite of approximate An_{60} composition, which is relevant to martian basaltic shergottites and eclogites.

METHODS

Synthesis

We performed high-pressure, high-temperature experiments coupled with in situ energy dispersive X-ray diffraction and imaging at the Argonne National Laboratory Advanced Light Source using the large volume multi-anvil press with a D-DIA apparatus available on the 6-BM-B beamline. The possible effects of crystallinity of the precursor were tested by using two different starting materials, a natural crystalline plagioclase feldspar powder of approximate labradorite composition ($An_{59.25}Ab_{39.25}Or_{1.5}$), originating from Chihuahua, Mexico, and provided by Byrne et al. (2015), and an amorphous powder with the same composition. The amorphous material was a fused glass synthesized using the natural labradorite powder and heated in a Deltec Furnace to ~1500 °C in a sealed Pt capsule for 2 h and quenched in air. The composition used here is consistent with the average composition of natural tissintite (Ma et al. 2015).

Each sample was loaded into a high-pressure cell assembly (Fig. 1), with mullite as the pressure medium and a graphite furnace. The pressure and temperature were monitored using a MgO pressure calibrant and a W3%Re–W25%Re alloy thermocouple. The samples were cold compressed at ambient temperature to peak pressure followed by heating. We utilized two different heating protocols: (1) a stepped heating method where the temperature was increased by 200 °C every 60 s and (2) a spike heating method where the sample was elevated to peak temperature within ~1 s, followed by a rapid quench after 60 s at peak temperature. The spike heating method was meant to loosely mimic the rapid temperature increase and decrease that material would experience when adjacent to melts produced during an impact event. While shock melts can reach up to 2500 °C or higher, this is not necessarily the temperature materials reach when heated through conduction when in contact with melt, thus the target peak temperature range for these experiments was 1200–1400 °C, which is comparable to temperatures estimated for materials in contact with shock melts (Langenhorst and Poirier 2000; Walton et al. 2006, 2016; Shaw and Walton 2013; Ma et al. 2015).

Energy-dispersive X-ray diffraction patterns for the sample and the pressure calibrant were collected by solid-state Ge detectors. The incident X-ray beam was collimated to $100 \times 100 \mu\text{m}$ for diffraction. Though the spectra from only a single detector are shown in the later figures for simplicity, beamline 6-BM-B is equipped with a 10-element detector array with the individual elements oriented in a circular array. A series of two conical slits then fixes the 2θ of the diffracted X-ray beam at 6.50° for all 10 detector elements. The conditions at which diffraction data were collected for each sample are shown in Figures 2 to 5.

Recovered sample analysis

The samples were recovered as dense pellets ~2 mm in diameter and ~0.5 to 1 mm in thickness. A portion of each was embedded in epoxy, thinly sliced and polished to produce thick sections, ~100–200 μm thick. These samples were analyzed using micro-Raman spectroscopy. Raman spectra were collected using a WiTec Alpha 300R confocal imaging system equipped with a 532 nm Nd:YAG laser available in the Center for Planetary Exploration (CPeX) at Stony Brook University. All spectra were collected through a $50\times$ (NA = 0.85) objective with a

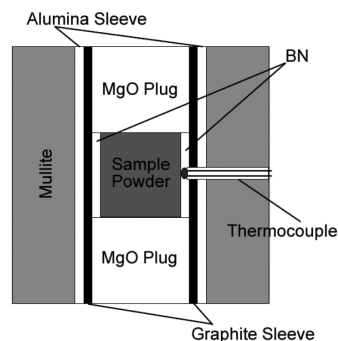


FIGURE 1. Cross-section view of the standard cell assembly used in these experiments.

working spot size of $0.76 \mu\text{m}$. Each spectrum is an accumulation of 60 scans with an integration time of 1 s.

RESULTS AND DISCUSSION

The progression of the in situ diffraction patterns for three experimental runs denoted as L01, L02, and L03, respectively, are shown in Figures 2–4. Each run tested three different sets of conditions that, along with the experimental outcomes, are summarized in Table 1. During cold compression, no new phases were observed in both the crystalline and amorphous starting material. The apparent broadening and disappearance of diffraction peaks for the crystalline material during compression shown in Figures 2 and 3 is consistent with partial amorphization and/or differential stress distribution (Miyahara et al. 2013). We observed the formation of tissintite only after heating in all three experiments, where the diffraction pattern is consistent with a jadeite-like structure. The formation of tissintite occurred via solid-state reaction as the temperatures tested in all three experiments are below the liquidus for labradorite and no melting was observed. In Figures 2 to 4, the prominent diffraction peaks associated with each phase are labeled; tissintite is denoted by the prominent doublet features between 2 and 3 Å. Representative Raman spectra for each recovered sample

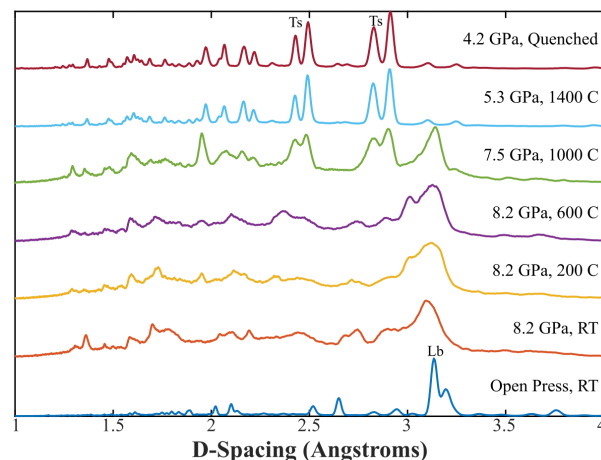


FIGURE 2. Formation of tissintite (Ts) from crystalline labradorite (Lb) at 7.5 GPa and >1000 °C using stepped heating. The prominent peaks of each phase are labeled. (Color online.)

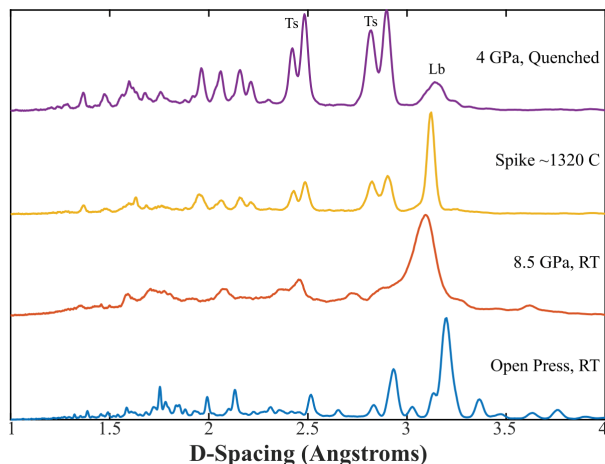


FIGURE 3. Formation of tissantite (Ts) from crystalline labradorite (Lb) at 8.5 GPa and 1320 °C using spike heating. The prominent peaks of each phase are labeled. (Color online.)

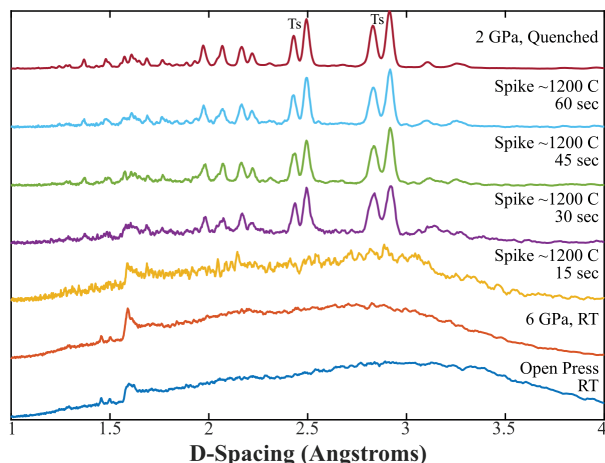


FIGURE 4. Formation of tissantite (Ts) from amorphous labradorite at 6 GPa and 1200 °C using spike heating. The prominent peaks of each phase are labeled. (Color online.)

are shown in Figure 5 along with a spectrum of natural tissantite for comparison provided by C. Ma (personal correspondence). Raman peak positions for each sample and natural tissantite are shown in Table 2.

In run L01, where the crystalline starting material was compressed to 8.5 GPa and step heated to 1400 °C, tissantite began to crystallize at ~1000 °C and the crystalline material was completely converted to tissantite at 1400 °C. However, in run L02 where crystalline labradorite was spike heated, we observed remaining crystalline labradorite in both the in situ diffraction patterns and in the Raman spectrum. Figure 6 shows a reflected light image of a labradorite grain within the recovered sample from run L02. In this sample, an apparent “rind” of tissantite that has formed along the edges of the labradorite grain can be seen. In the natural setting, tissantite can form as a rind along the edges of a maskelynite grain that are abutting or entrained in shock melt (Ma et al. 2015). While both occurrences appear

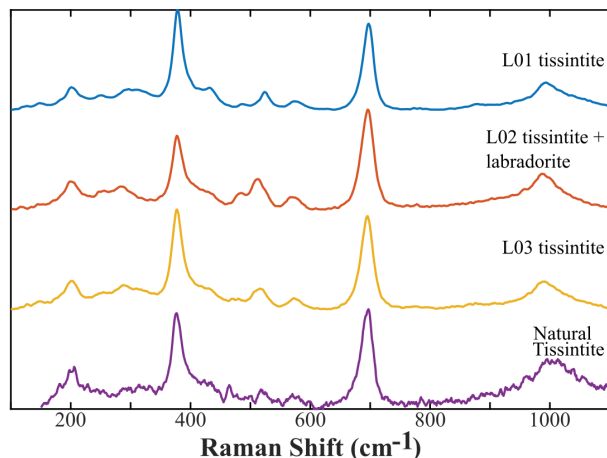


FIGURE 5. Representative spectra for each run compared to data for natural tissantite (Ma et al. 2015). The three major peaks for tissantite are 377, 693, and 1003 cm^{-1} . Synthetic tissantite from this study shows remarkable agreement with natural tissantite, confirming its synthesis. (Color online.)

similar, the textural contexts are different. Besides the remnant labradorite, no other coexisting crystalline phases were identified in either the diffraction or the spectral data.

In addition, we observed the crystallization of tissantite as a function of time during the spike heating of the amorphous material by collecting an average diffraction pattern in 15 s intervals during the 60 s spike. Tissantite begins to nucleate within the first 15 s. While the major tissantite doublet peaks are not apparent in the diffraction pattern for the first 15 s at temperature (Fig. 3), the limits of the technique make it likely that the peaks are masked by noise at the beginning of nucleation, rendering them indiscernible until after the crystals have grown above a certain size. In similar experiments reported by Kubo et al. (2010), crystallization of a jadeite-like material was observed in labradorite at 12.6 GPa and 930 °C after ~10 s. While our experiments are performed at temperatures closer to a shock event, there could be a lag during spike heating from ambient to peak temperature where the center of the sample does not reach peak temperature for the first 2–3 s.

TABLE 1. Experimental runs and outcomes

Run no.	Starting material	Peak P (GPa)	Peak T (°C)	Heating method	Product
L01	Crystalline	8.2	1400	Step	tissantite
L02	Crystalline	8.5	1320	Spike	tissantite + labradorite
L03	Amorphous	6	1200	Spike	tissantite

TABLE 2. Raman shift peak positions for synthetic tissantite (this study) and natural tissantite (Ma et al. 2015)

L01	L02	L03	Natural tissantite
202	200	203	203
378	377	378	377
432	437	433	417
–	485 ^a	–	–
–	512 ^a	–	–
524	–	517	518
573	–	574	573
698	696	696	693
993	987	990	1003

^aLabradorite peaks.

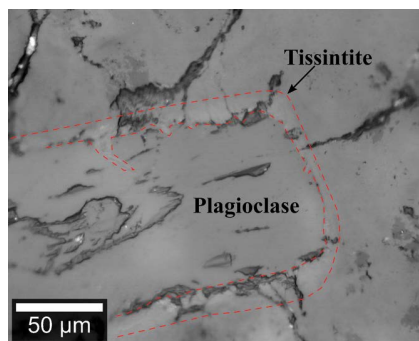


FIGURE 6. In this reflected light image a light halo of tissintite is evident around a large plagioclase grain within L02. This texture is reminiscent of that observed in natural tissintite samples. (Color online.)

IMPLICATIONS

We have found that tissintite readily forms under the following range of conditions: 6–8 GPa and 1000–1350 °C. While the temperatures are similar to those estimated for materials in contact with shock-generated melts in basaltic materials (Langenhorst and Poirier 2000; Shaw and Walton 2013), the pressures are low relative to maskelynite formation pressures of ~29 GPa (Stöffler et al. 1986; Fritz et al. 2017). Furthermore, through our novel spike heating protocol we observed that heating at shock-like time scales is not sufficient to convert crystalline labradorite to tissintite. This observation is significant as it clearly indicates that in the natural case, where tissintite is only seen in conjunction with maskelynite (amorphous plagioclase), the crystalline plagioclase had to become amorphous before contact with shock melt to produce tissintite with no coexisting crystalline plagioclase or other phases. This not only gives us an idea of when during the impact event tissintite began to form, but also when maskelynite forms as well. Thus, tissintite likely forms during decompression from an amorphous plagioclase precursor that became amorphous during compression in the same event or became amorphous during a previous impact event.

ACKNOWLEDGMENTS

The authors acknowledge the constructive reviews of Chi Ma, John Spray, Oliver Tschauner, and Erin Walton that helped to improve the manuscript. The authors thank Donald Lindsley (SBU) and Hanna Nekvasil (SBU) for help with the synthesis of starting materials. Portions of this research were supported by the NASA Earth and Space Science Fellowship program and the RIS4E node of NASA's Solar System Exploration Research Virtual Institute. Use of the Advanced Photon Source, Argonne National Laboratory, was supported by the U.S. Department of Energy, Office of Science, Office of Basic Energy Sciences, under Contract No. DE-AC02-06CH11357. Use of the 6-BM-B beamline was supported by COMPRES, the Consortium for Materials Properties Research in Earth Sciences, under NSF Cooperative Agreement EAR 16-06856 and by the Mineral Physics Institute, Stony Brook University. MPI Publication 509.

REFERENCES CITED

Boonsue, S., and Spray, J.G. (2017) Shock-generated labradorite polymorphs in terrestrial impact rocks at Manicouagan. *Lunar and Planetary Science XLVIII*, abstract 2557.

- Byrne, S.A., Dyar, M.D., Bessette, E.E., Breitenfeld, L.B., Crowley, M.C., Hoff, C.M., Marchand, M.N., Ketley, M.N., Roberts, A.L., Sklute, E.C. and Parente, M. (2015) Pure mineral separates for mixing experiments to simulate planetary surfaces. *Lunar and Planetary Science XLVI*, abstract 1499.
- Chen, M., and El Goresy, A. (2000) The nature of maskelynite in shocked meteorites: not diaplectic glass but a glass quenched from shock-induced dense melt at high pressures. *Earth and Planetary Science Letters*, 179, 489–502.
- Chen, M., Sharp, T., El Goresy, A., Wopenka, B., and Xie, X. (1996) The majorite-pyroxene + magnesiowüstite assemblage: Constraints on the history of shock veins in chondrites. *Science*, 271, 1570–1573.
- Fritz, J., Greshake, A., and Fernandes, V. (2017) Revising the shock classification of meteorites. *Meteoritics and Planetary Science*, 1–17.
- Gillet, P., El Goresy, A., Beck, P., and Chen, M. (2007) High-pressure mineral assemblages and shocked terrestrial rocks: Mechanisms of phase transformations and constraints to pressure and temperature histories. In E. Ohtani, Ed., *Advances in High-Pressure Mineralogy*, 421, p. 57–82. Geological Society of America Special Paper.
- Herd, C., Walton, E., Agee, C., Muttik, N., Ziegler, K., Shearer, K., Bell, A., Santos, A., Burger, P., Simon, J., and others. (2017) The Northwest Africa 8159 martian meteorite: Expanding the martian sample suite to the early amazonian. *Geochimica et Cosmochimica Acta*, 1–26.
- Langenhorst, F., and Poirier, J. (2000) Anatomy of black veins in Zagami: Clues to the formation of high-pressure phases. *Earth and Planetary Science Letters*, 184, 37–55.
- Kubo, T., Kimura, M., Kato, T., Nishi, M., Tominaga, A., Kikegawa, T., and Funakoshi, K. (2010) Plagioclase breakdown as an indicator for shock conditions of meteorites. *Nature Geoscience Letters*, 3, 41–45.
- Ma, C., Tschauner, O., Beckett, J., Liu, Y., Rossman, G., Zuravlev, K., Prakupenka, V., Dera, P., Sinogeikin, S., Smith, J., and Taylor, L. (2014) First new minerals from Mars: discovery of Ahrensite γ -Fe₂SiO₄ and tissintite (Ca,Na,□)AlSi₂O₆, two high pressure phases from the tissintite Martian meteorite. 45th Lunar Planetary Science Conference, Abstract 1222.
- Ma, C., Tschauner, O., Beckett, J., Liu, Y., Rossman, G., Zuravlev, K., Prakupenka, V., Dera, P., and Taylor, L. (2015) Tissintite, (Ca,Na,□)AlSi₂O₆, a highly defective, shock-induced, high-pressure clinopyroxene in the Tissintite martian meteorite. *Earth and Planetary Science Letters*, 422, 194–205.
- Miyahara, M., Ozawa, S., Ohtani, E., Kimura, M., Kubo, T., Sakai, T., Nagase, T., Nishijima, M., and Hirao, N. (2013) Jadeite formation in shocked ordinary chondrites. *Earth and Planetary Science Letters*, 373, 102–108.
- Ohtani, E., Kimura, Y., Kimura, M., Takata, T., Kondo, T., and Kubo, T. (2004) Formation of high-pressure minerals in shocked L6 condrite Yamato 791384: constraints on shock conditions and parent body size. *Earth and Planetary Science Letters*, 277, 505–515.
- Pang, R., Zhang, A., Wang, S., Wang, R., and Yurimoto, H. (2016) High-pressure minerals in eucrite suggest a small source crater on Vesta. *Scientific Reports*, 6, 26063.
- Sharp, T., and DeCarli, P. (2006) Shock effects in meteorites. *Meteorites and the Early Solar System II*, 653–677.
- Shaw, C., and Walton, E. (2013) Thermal modeling of shock melts in Martian meteorites: Implications for preserving martian atmospheric signatures and crystallization of high-pressure minerals from shock melts. *Meteoritics and Planetary Science*, 48, Nr. 5, 758–770.
- Stöffler, D., Ostertag, R., Jammes, C., Pfannschmidt, G., Sen Gupta, P.R., Simon, S.B., Papike, J.J., and Beauchamp, R.H. (1986) Shock metamorphism and petrography of the Shergotty achondrite. *Geochimica et Cosmochimica Acta*, 50, 889–903.
- Walton, E., Shaw, C., Cogswell, S., and Spray, J. (2006) Crystallization rates of shock melts in three martian basalts: Experimental simulation with implications for meteoroid dimensions. *Geochimica et Cosmochimica Acta*, 70, 1059–1075.
- Walton, E., Sharp, T., Hu, J., and Filiberto, J. (2014) Heterogeneous mineral assemblages in martian meteorite Tissint as a result of a recent small impact event on mars. *Geochimica et Cosmochimica Acta*, 140, 334–348.
- Xie, Z., Sharp, T., and DeCarli, P. (2006) High-pressure phases in a shock-induced melt vein of the Tenham L6 chondrite on shock pressure and duration. *Geochimica et Cosmochimica Acta*, 70, 504–515.

MANUSCRIPT RECEIVED MARCH 6, 2018

MANUSCRIPT ACCEPTED MAY 17, 2018

MANUSCRIPT HANDLED BY IAN SWAINSON